Insights into the role of the (α+β) insertion in the TIM-barrel catalytic domain, regarding the stability and the enzymatic activity of Chitinase A from Serratia marcescens

ARTICLE *in* BIOCHIMICA ET BIOPHYSICA ACTA · NOVEMBER 2008

Impact Factor: 4.66 · DOI: 10.1016/j.bbapap.2008.09.018 · Source: PubMed

3 AUTHORS, INCLUDING:

Serapion Pyrpassopoulos
University of Pennsylvania
14 PUBLICATIONS **160** CITATIONS
SEE PROFILE

Constantinos E Vorgias
National and Kapodistrian University of Ath…
92 PUBLICATIONS **3,007** CITATIONS
SEE PROFILE

Biochimica et Biophysica Acta 1794 (2009) 23–31

Contents lists available at ScienceDirect

Biochimica et Biophysica Acta

journal homepage: www.elsevier.com/locate/bbapap

Insights into the role of the (α+β) insertion in the TIM-barrel catalytic domain, regarding the stability and the enzymatic activity of Chitinase A from *Serratia marcescens*

Athanassios C. Zees [a], Serapion Pyrpassopoulos [b,c], Constantinos E. Vorgias [a,*]

[a] National and Kapodistrian University of Athens, Faculty of Biology, Department of Biochemistry and Molecular Biology, Panepistimiopolis-Zographou, 15784 Athens, Greece
[b] Biomolecular Physics Laboratory, I/R-RP, National Centre for Scientific Research "Demokritos", 15310 Aghia Paraskevi, Greece
[c] Pennsylvania Muscle Institute, Department of Physiology, University of Pennsylvania School of Medicine, B400 Richards Building, 3700 Hamilton Walk, Philadelphia, PA 19104, USA

ARTICLE INFO

Article history:
Received 1 March 2008
Received in revised form 16 September 2008
Accepted 17 September 2008
Available online 10 October 2008

Keywords:
Chitinase
Serratia
TIM-barrel insertion
Enzyme engineering
Protein modelling
Thermodynamics

ABSTRACT

Chitinase A (ChiA) from *Serratia marcescens* is a mesophilic enzyme with high catalytic activity and high stability. The crystal structure of ChiA has revealed a TIM-barrel fold of the catalytic domain, an (α+β) insertion between the B7 β-strand and A7 α-helix of the TIM-barrel, an FnIII domain at the N-terminus of the molecule and a hinge region that connects the latter to the catalytic domain. In this study, the role of the (α+β) domain on the stability, catalytic activity and specificity of the enzyme was investigated by deleting this domain and studying the enzymatic and structural properties of the resulting truncated enzyme. The obtained data clearly show that by removing the (α+β) domain, the thermal stability of the enzyme is substantially reduced, with an apparent T_m of 42.0±1.0 °C, compared to the apparent T_m of 58.1±1.0 °C of ChiA at pH 9.0. The specific activity of ChiAΔ(α+β) was substantially decreased, the pH optimum was shifted from 6.5 to 5.0 and the substrate and product specificities were altered.

1. Introduction

Chitin is a linear insoluble polysaccharide and one of the most abundant in nature, second only to cellulose, which consists of N-acetyl-β-D-glucosamine (NAG) residues connected via β(1,4) linkages [1]. Chitin is not only a major constituent of the fungal cell wall and of the arthropod exoskeleton, but also an important nutrient source for bacteria. In nature, chitin can be found in three structural forms. The most common, α-chitin, is amorphous and characterized by an antiparallel arrangement of adjacent chains, whereas β-chitin is crystalline and characterized by a parallel arrangement of adjacent chains. The third structural form, γ-chitin, is a mixture of α and β-chitin. Chitin and its chemically modified derivatives exhibit antimicrobial, antitumor and wound healing physiological activities, among others. Chitin is a valuable biomaterial due to its excellent biocompatibility and biodegradability [2]. Over 100 billion tons of raw material of this biopolymer are being naturally recycled in our biosphere, annually [3].

Chitinases [EC 3.2.1.14] are nature's most efficient countermeasure to chitin accumulation. These enzymes comprise families 18 and 19 of the glycosyl hydrolases superfamily, based on the similarity of their primary structures [4,5]. Family 19 is generally highly conserved and contains mainly plant chitinases and some of the characterized chitinolytic enzymes from the Gram-positive bacterium *Streptomyces sp* [6,7]. On the other hand, family 18 includes a large number of diversely evolved chitinases from plants, animals, bacteria and fungi which have been identified either as endochitinases or as exochitinases [8]. The first group randomly cleaves the chitin chain, whereas the second group cleaves chitobiose, $(NAG)_2$, or chitotriose, $(NAG)_3$, from the reducing or the non-reducing end of the chitin chain, processively [9–11].

Serratia marcescens is a Gram-negative soil bacterium, belonging to the family *Enterobacteriaceae* [12], that mobilizes an effective chitinolytic weaponry to utilize chitin as a nutrient source. It is an intensively studied microorganism, mainly due to its potential application in biological control [13,14]. In that respect, the bacterium produces three different secreted chitinases with distinct activities, ChiA, ChiB and ChiC, as well as a β-N-acetyl-D-hexosaminidase (chitobiase, Chb) [EC 3.2.1.52] and a chitin binding protein, CBP21 [15–18]. All three chitinases belong to family 18 and they possess a TIM-barrel fold as their catalytic domain. The TIM-barrel fold is a versatile structural scaffold for more than 40 different enzyme specificities [19,20].

Family 18 chitinases can be divided into three subfamilies A, B, and C, in terms of the primary structure similarity of their catalytic domains [21]. The major structural difference, deduced from the amino acid sequence comparison between subfamilies A and B, reveals that ChiA and ChiB of subfamily A have an inserted domain between the seventh and eighth β-strands of the TIM-barrel catalytic

* Corresponding author. Tel.: +30 210 7274514; fax: +30 210 7274158.
E-mail address: cvorgias@biol.uoa.gr (C.E. Vorgias).

1570-9639/$ – see front matter © 2008 Elsevier B.V. All rights reserved.
doi:10.1016/j.bbapap.2008.09.018

domain, while this insertion is absent in ChiC, a member of subfamily B chitinases. [15]. ChiA, in particular, has an insertion of 75 amino acid residues, with an (α+β) fold, between strand B7 and helix A7 [22–24]. The function of the inserted (α+β) domain, with regard to the biophysical and enzymatic properties of ChiA, is not yet known. The results of current studies suggest that this insertion in subfamily A chitinases may be partially responsible for the exochitinase activity and processivity of these enzymes. [15,25–29]. Therefore, it is of particular interest to elucidate the function of this structural domain. In the present work, we focussed on some of the effects that the removal of the (α+β) domain causes on the stability, specificity and catalytic activity of the ChiA enzyme by employing genetic engineering, thermodynamics and biocomputing.

2. Materials and methods

Luria–Bertoni broth and antibiotics were purchased from Sigma. Restriction enzymes and T4 ligase were from New England Biolabs. Taq DNA polymerase (platinum-high fidelity) was from InVitrogen. Fluorescent substrates, 4-Methyl-Umbeiliferyl-(N-acetyl-β-D-glucosamine)$_2$ (4MU(NAG)$_2$) and 4-Methyl-Umbeiliferyl-(N-acetyl-β-D-glucosamine)$_3$ (4MU(NAG)$_3$), as well as chitin and chitooligosaccharides (from NAG to (NAG)$_7$),were purchased from Sigma. Bradford reagent was from Biorad. ECL (electro-chemical luminance) substrate for horseradish peroxidase was purchased from Amersham. All other chemicals, salts and substances used, were of the highest analytical grade (Sigma, Merck).

2.1. Construction and cloning of the *chiA* and the *chiAΔ(α+β)* genes

The *chiA* gene, originally isolated from *S. marcescens* by Jones et al. [30], was cloned into the pCR2.1 vector (InVitrogen) following the current cloning procedures as described in Sambrook et al. [31]. The expression of the *chiA* gene, from strain QMB1466, was also carried out as described in previous publication [24].

The *chiAΔ*(α+β) gene was constructed from the *chiA* gene by applying pcr-fusion technology and was then cloned into the pCR2.1 vector. A typical pcr reaction of 50 μl final volume, contains the following components at final concentrations: template DNA 20 ng/μl, N/C primers 1 μM each, dNTPs 200 μM each, Amplitaq DNA polymerase 0.025 U per μl, 10 mM Tris–HCl pH 8.3 (at 25 °C), 50 mM KCl, 0.01%(w/v) gelatine and 0.5–2.0 mM total $MgCl_2$. The pcr-fusion experiment comprises 2 pairs of primers in two separate reactions, using the *chiA* gene cloned into the pCR2.1 vector as the template. The first reaction involved the M13 reverse primer from pCR2.1 as the N-primer and the 21-mer oligonucleotide ATGGCCGCGGCGGCACCTTCG (oligo-A), as the C-primer. The oligo-A has its first 11 bases identical to the *chiA* gene sequence from 1331 to 1341 bp and its last 7 bases identical to the *chiA* gene sequence from 1537 to 1543 bp. Between these two regions, a GGC codon was inserted (underlined in oligo-A), which encodes for a glycine residue. In the second reaction, the 21-mer oligonucleotide CGAAGGTGCCGCCGCGGCCAT, which is antiparallel to oligo-A, was used as the N-primer, while the C-primer was the M-13 forward primer from pcr2.1. The pcr reactions were performed using a Stratagene RoboCycler device for 30 cycles, with the following steps per cycle: denaturation at 94 °C for 1 min, annealing at 50–60 °C for 1 min and polymerization at 72 °C for 2 min. Ten μl of the amplification mixture was normally analyzed by 1% agarose in TBE buffer (89 mM Tris base, 89 mM boric acid, 2 mM EDTA) at 80–100 V constant voltage and stained with ethidium bromide. Both pcr products were then purified using the QIAquick PCR purification kit (Qiagen). The purified products were combined in equal molarities. To achieve the desired fusion the mixture of the pcr products was melted at 94 °C and annealed at 65 °C, several times. The annealed combined fragments were used as templates for the amplification procedure, by using the M13 reverse primer and the M13 forward primer as the N and C-primers, respectively. Upon these conditions, we obtained the *chiA-Δ*(α+β) gene, which is the *chiA* deleted from 1342 to 1536 bp, with a simultaneous insertion of the GGC codon at position 1342. The amplified gene was introduced into the pCR2.1 vector and verified by DNA sequencing according to the dideoxy chain termination method [32].

In order to express the *chiA* and *chiAΔ*(α+β) genes, the pET-15b expression vector (Novagen) was used. Both vector and inserts were digested with NcoI–BamHI and ligated to create the pET-15b-*chiA* and pET-15b-*chiAΔ*(α+β) expression constructs, which were verified by sequencing. The pET-15b-*chiA* expression vector was introduced into the AD494(DE3)pLysS (Novagen), while the pET-15b-*chiAΔ*(α+β) was introduced in the AD494(DE3) (Novagen) expression host cells for ChiA and ChiAΔ(α+β) protein overproduction, respectively [33]. In both constructs, the original signal peptide of ChiA, at the N-terminus of the protein, was removed and replaced by a Tag of 6xHis, to facilitate rapid purification.

2.2. Overproduction and purification of the ChiA and the ChiAΔ(α+β) proteins

ChiA was overproduced and purified to homogeneity based on the following procedure developed in our laboratory. Briefly, in a routine protein preparation, a 6.0 litre 0.6–0.7 $OD_{600\ nm}$ cell culture was induced with 1 mM IPTG for 3 h at 25 °C. The bacteria were collected by low speed centrifugation in a Sorval SLA-1500 rotor at 8000 rpm for 10 min and washed once with ice cold PBS buffer (10 mM Na_2HPO_4, 1.8 mM KH_2PO_4, 140 mM NaCl, 2.7 mM KCl). All further procedures were carried out at 4 °C, unless otherwise specified. The bacterial paste was resuspended in 10 ml/g buffer A (Buffer A: 20 mM Na-phosphate pH 8.0, 10 mM imidazole, 0.1 mM PMSF, 100 mM NaCl, 0.1% (w/v) Triton X-100). The cells were disrupted by sonication for 20 min and the extract was clarified by centrifugation in a Sorvall SS-34 rotor at 15,000 rpm for 30 min. The supernatant was applied on a 5 ml HighTrap Chelating column (Pharmacia) charged with Ni^{2+}. Bound proteins were eluted between 100 and 300 mM imidazole of a linear ascending gradient of 50 ml total volume and 2 ml fractions were collected. Fractions highly enriched in ChiA were combined, adjusted to 0.5 M ammonium sulphate and applied on a 5 ml Butyl-TSK column (Merck) equilibrated in Buffer B (20 mM Na-phosphate pH 8.0, 1 M ammonium sulphate). Bound proteins were eluted between 500 and 0 mM ammonium sulphate, of a linear descending gradient of 100 ml total volume and 2 ml fractions were collected. In both cases, the collected fractions were analyzed by 0.1%SDS–12%PAGE, using the Broad range prestained Protein Molecular Weight Marker (New England Biolabs).

ChiAΔ(α+β) was overproduced and purified to homogeneity following a similar procedure, except that the induction temperature was 18 °C and the Butyl-TSK column was omitted.

Prior to proceeding to further experimental analysis, both purified enzymes were treated with thrombin (0.01 mg/mg of protein) for 1 h at 37 °C and pH 7.6, to remove the Tag peptide of 6xHis from the N-terminus of the proteins. The reaction mixture was then dialyzed against Buffer A and reapplied to the Ni^{2+}-HighTrap Chelating column to remove the free Tag of 6xHis.

2.3. Protein detection and verification

Protein analysis was carried out in 0.1%SDS–12%PAGE as described by Laemmli [34]. Protein concentration was determined either by the Bradford method [35], or from the molar extinction coefficient at 280 nm. The molar extinction coefficient of ChiA and ChiAΔ(α+β) was calculated, from their primary structure, to be 107,050 and 83,100 M^{-1} cm^{-1}, respectively [36,37]. Western Blot analysis of both ChiA and ChiAΔ(α+β) was performed, using rabbit polyclonal anti-

ChiA as the first antibody and anti-rabbit horseradish peroxidase as the second [31,38]. The results were visualized on photographic film by applying electro chemical luminance (ECL).

2.4. Circular dichroism spectroscopy (CD)

CD measurements were conducted using a Jasco-715 spectropolarimeter equipped with a Peltier type cell holder (PTC-348WI), for temperature control. Wavelength scans in the far (190 to 260 nm) and near UV region (250 to 320 nm) were performed in Quartz SUPRASIL (HELLMA) precision cells of 0.1 cm and 1 cm path length, correspondingly. Each spectrum was obtained by averaging five to ten successive accumulations with a wavelength step of 0.2 nm at a rate of 50 nm/min, response time 2 s and band width 1 nm. Thermal CD experiments were carried out from 15 °C to 75 °C, at 222 nm and heating scan rate 1.5 K/min. In all cases, protein concentration within the range of 0.5 and 1 mg/ml was used in 50 mM Tris–HCl pH 9.0 buffer.

2.5. High-precision differential scanning calorimetry (DSC)

Calorimetric measurements were performed on a VP-DSC microcalorimeter (MicroCal) at a heating rate of 1.5 K/min using protein concentration within the range of 0.5 and 1 mg/ml. All samples were degassed prior to use and 4 to 5 thermal scans, with buffer-filled cells to ensure baseline reproducibility, preceded each sample run. The samples were in 50 mM Tris–HCl pH 9.0 buffer and measured twice.

2.6. Enzyme assays

Chitinase activity measurements on fluorescent substrates [26,39,40] were performed in 96-well, black Elisa plates, with 350 μl capacity per well and flat-bedded bottom surface, from BMG Labtech, to a final volume of 100 μl. The spectrofluorometer used for collecting real time kinetic data in various temperatures (25–45 °C, with 5 °C steps) was a BMG Fluostar Galaxy microplate reader. All the enzymatic reaction components, except the enzyme, were preheated at each temperature for 5 min, followed by addition of the enzyme. This procedure was applied anew for every temperature step and data were collected successively, every 15 s per well, for a maximum of 1 h. Various concentrations of 4MU$(NAG)_2$ and 4MU$(NAG)_3$, from 0.5 μM to 100 μM, were used as substrates for chitinases in a pH range from 4.0 to 9.0 (4.0–5.5 Na-acetate, 6.0–8.0 Na-phosphate, 8.5–9.0 Tris–HCl) and at 50–100 mM NaCl. The excitation wavelength employed for the 4MU product was 355 nm and the emission wavelength selected was 450 nm. The instrument sensitivity was adjusted between gain 60 and 70, after detailed calibration. Temperature profile measurements were carried out at the optimum pH of each enzyme, 6.5 for ChiA and 5.0 for ChiAΔ(α+β), whereas pH profile data were obtained at the optimum temperature for each enzyme, 45 °C for ChiA and 35 °C for ChiAΔ(α+β). The kinetics for both enzymes were calculated from initial rate, real time data, to avoid extended pH and temperature effects on the stability of the two proteins.

2.7. Analysis of hydrolysis products of various chitinous polymers

Hydrolysis products arising from the ChiAΔ(α+β) action were determined using colloidal chitin and synthetic substrates. Oligosaccharides derived from chitin are β-(1,4)-linked oligomers of NAG and are designated: $(NAG)_2$ for β-(1,4)-N,N′-di(acetyl)-chitobiose; $(NAG)_3$, $(NAG)_4$, $(NAG)_5$, $(NAG)_6$ and $(NAG)_7$ for the corresponding chitotriose, chitotetraose, chitopentaose, chitohexaose and chitoheptaose. ChiAΔ(α+β) (350 μg/ml) was incubated with 1 mg/ml of synthetic oligosaccharides in 20 mM Na-acetate (pH 5.0) at 25 °C, for up to 48 h. In the case of colloidal chitin, 350 μg/ml of ChiAΔ(α+β) was incubated with 1 mg/ml of substrate in 20 mM Na-acetate (pH 5.0) at 25 °C, for up to 48 h also. ChiA was also incubated, using a concentration of 50 μg/ml, with a corresponding amount of colloidal chitin, in 20 mM Na-phosphate (pH 6.5), at 37 °C, for 12 h. The hydrolysis products were analyzed by high performance liquid chromatography (HPLC) (reverse phase, aminopropyl-silica column, μ-Bondapak, 125A, Waters). The sugars were isocratically eluted with 75% acetonitrile in ddH_2O at a rate of 1.5 ml/min and at room temperature. The separated products were detected by refractive index at 210 nm and compared to standard chitooligosaccharides.

2.8. Methods in silico

The theoretical pIs of the two proteins were calculated using the pI** program available online on the EMBL Computational Services site (www.embl-heidelberg.de/cgi/pi-wrapper.pl). Bioinformatics analysis of the two enzymes was carried out using the ClustalX software for sequence alignment [41] and the MODELLER 9v2 software [42] for molecular modelling. The structure of ChiA was superimposed with the C_a atom on the structure of ChiB and a structural alignment was obtained with the DALI software [43]. Potential hydrogen bonds and salt bridges were detected by using the WHAT IF software package [44]. The electrostatic densities, located in the region of the deletion, were designed by the GRASP2 software [45]. Contributions to pKa values were predicted using the H+ software (available online at the URL http://biophysics.cs.vt.edu/H+) and applying the Poisson–Boltzmann equation. The ChiA and ChiAΔ(α+β) structures were visualized and compared with the PYMOL software (DeLano Scientific LLC, Palo Alto, USA).

3. Results

Based on detailed inspection of the ChiA structure, specifically focussing on the area of the (α+β) domain, we decided to remove the respective amino acid sequence (65 residues, 448–512 aa) and insert a glycine residue, immediately after the amino acid G447 of ChiA. The pcr-fusion approach successfully afforded the *chiAΔ*(α+β) gene, which is the *chiA* deleted from 1342 to 1536 bp and an insertion of a GGC codon (glycine) was simultaneously added at 1342 bp, as described in the Materials and methods.

The recloning procedure into the pET-15b expression vector for heterologous protein overproduction added a Tag of 6 histidines and an incorporated thrombin cleavage site (underlined in the following amino acid sequence: $MGSSH_6SSGLVPRGSH$) to ChiA and ChiAΔ(α+β), attached to their N-termini. The addition of the 20 amino acid residue long oligopeptide shifted the molecular weight of ChiA (aa=540) and ChiAΔ(α+β) (aa=476) by 2.2 kDa to 63.2 and 55.8 kDa, respectively. The purification scheme of both enzymes, as described in the Materials and methods, resulted in an overall yield of 12 mg of highly purified ChiA (Fig. 1, lane 1) and 15 mg of highly purified ChiAΔ(α+β) (Fig. 1, lane 2) protein from 6.0 l of bacterial cultures. Both purified proteins, ChiA and ChiAΔ(α+β), were verified by Western Blot, using rabbit polyclonal antibody raised against ChiA (Fig. 1, lanes 4 and 5). Concerning the solubility properties of the recombinant proteins, ChiA is soluble, highly active and structurally stable for several months at the pH range between 4.0 and 9.0 at 4 °C, whereas ChiAΔ(α+β) remains soluble, active and stable at the same pH range, at 4 °C, but only for one week. Both enzymes were stored in 20 mM Na-phosphate pH 8.0, 100 mM NaCl at 4 °C.

3.1. DSC thermal denaturation studies

The thermal denaturation of ChiA and ChiAΔ(α+β) was studied by high-precision differential calorimetry at pH 4.0, 7.0 and 9.0, at a buffer concentration of 50 mM, as described in the Materials and methods. The thermal denaturation for both proteins was irreversible at a pH range between 4.0 and 9.0. At pH 4.0 and 7.0, ChiA and

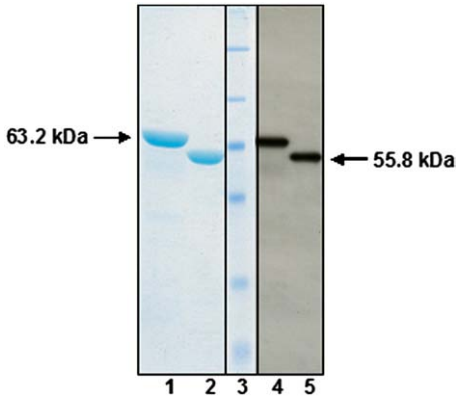

Fig. 1. 0.1%SDS–12%PAGE and Western Blot analysis of purified ChiA and ChiAΔ(α+β). ChiA (lane 1), ChiAΔ(α+β) (lane 2), molecular weight marker (lane 3), with MWs 175–83–62–47.5–32.5–25 kDa from top to bottom, respectively. Western Blot analysis of ChiA (lane 4) and ChiAΔ(α+β) (lane 5) on ECL film.

ChiAΔ(α+β) were severely affected by aggregation, while at pH 9.0 they were not. The DSC thermal denaturation data for both proteins, presented in Fig. 2 (upper panel), were obtained at scanning rate u=1.5°/min in 50 mM Tris–HCl pH 9.0, using protein concentration within the 0.5 and 1 mg/ml range.

The heat denaturation profile of ChiA, i.e. heat capacity at constant pressure vs. temperature (<ΔC_p> vs. T), (Fig. 2, upper panel), exhibits an endothermic irreversible transition at an apparent T_m of 60.7 °C (temperature at maximum <ΔC_p>). Irreversibility affects the sharpness of the heat capacity peak, thereby hindering a thermodynamic analysis and dissection of the melting profile into possible contributions (van't Hoff ratio). However, the experimental DSC profile can be well described by the two-state irreversible denaturation model N→D

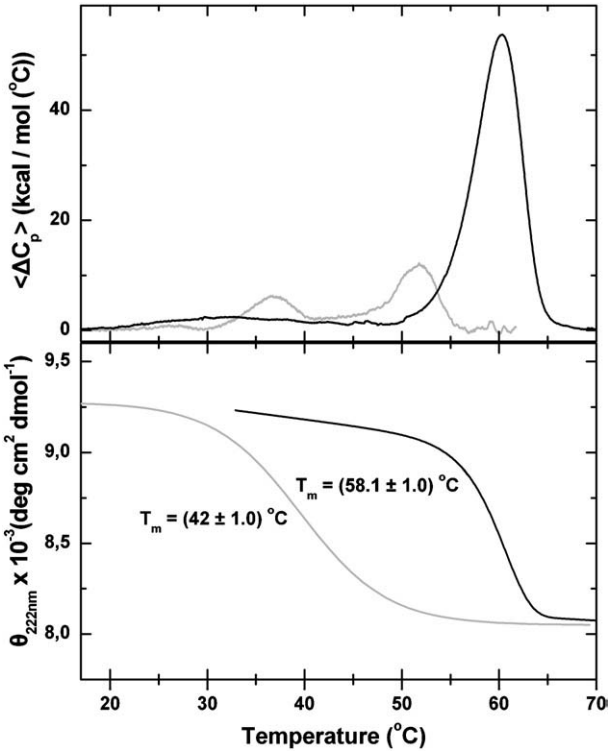

Fig. 2. Thermal stability studies of ChiA and ChiAΔ(α+β), employing DSC and CD at pH 9.0. Upper panel: DSC profiles for the heat-induced denaturation of ChiA (black line) and ChiAΔ(α+β) (grey line) (experimental details in the Materials and methods). Lower panel: The heat-induced denaturation of ChiA (black line) and ChiAΔ(α+β) (grey line) as recorded by the changes in ellipticity, θ, at λ=222 nm, via CD spectroscopy (experimental details in the Materials and methods).

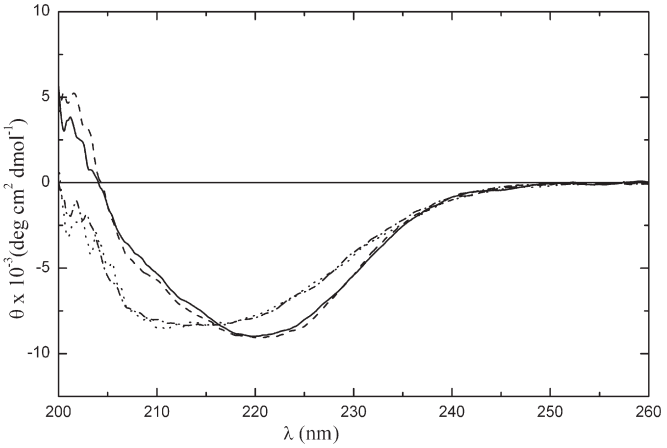

Fig. 3. Far-UV CD analysis of ChiA and ChiAΔ(α+β) at the native state (T=25 °C) and the denatured state (T=65 °C) at pH 9.0. Native ChiA (solid line), native ChiAΔ(α+β) (dashed line), denatured ChiA (dotted line) and denatured ChiAΔ(α+β) (dot-dashed line) (experimental details in the Materials and methods).

[Sanchez-Ruiz] [46,47]. In the case of ChiAΔ(α+β), thermal unfolding is also irreversible but more revealing and is characterized by two partially overlapping transitions, centered at about 38 °C and 52 °C (Fig. 2, upper panel). These data indicate that the thermal denaturation of ChiAΔ(α+β) proceeds via the unfolding of at least two distinct domains.

3.2. CD thermal denaturation studies

CD spectroscopy was employed to investigate and compare structural changes upon thermal unfolding of ChiA and ChiAΔ(α+β) proteins. CD experiments were carried out at pH 4.0, 7.0 and 9.0. However, pH 9.0 was ultimately used, for the same reason mentioned in the DSC section above. Deletion of the (α+β) domain from the ChiA protein bears no detectable effect on the far-UV CD spectrum of ChiA (Fig. 3). The near-UV spectrum is appreciably affected, since 3 tryptophan, 5 tyrosine and 3 phenylalanine residues were removed upon deletion of the (α+β) domain (from an overall of 14 tryptophans, 20 tyrosines and 25 phenylalanines), in addition to the fact that the packing density of the molecule may have also been affected (Fig. 4). Thus, impaired rigidity and compactness of the molecule, contributing to this difference in the near UV spectra, cannot be excluded.

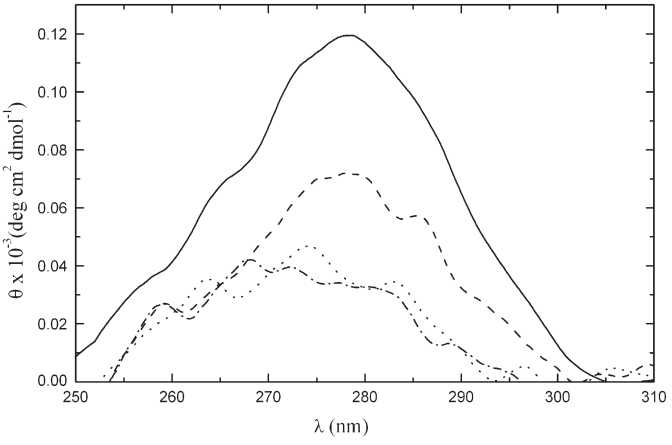

Fig. 4. Near-UV CD analysis of ChiA and ChiAΔ(α+β) at the native state (T=25 °C) and the denatured state (T=65 °C) at pH 9.0. Native ChiA (solid line), native ChiAΔ(α+β) (dashed line), denatured ChiA (dotted line) and denatured ChiAΔ(α+β) (dot-dashed line) (experimental details in the Materials and methods).

Thermal CD scans of ChiA at 222 nm exhibit a sharp transition centered at about 58 °C (Fig. 2, lower panel), a result that is in agreement to the DSC data (Fig. 2, upper panel). The corresponding melting profile of ChiAΔ(α+β) is not that steep and extends up to ~30 °C interval (from 30 °C to 60 °C), with a transition temperature T_m ~42 °C, indicating a much lower degree of cooperativity. This is also exhibited by the calorimetric results shown in Fig. 2 (upper panel). The removal of the (α+β) domain caused the melting point of the enzyme to drop by nearly 20 °C and the energy content to be reduced by nearly a factor of 3. Both differences provide evidence that the native enzyme is well-packed and thermally stable and demonstrates increased intradomain cooperativity, compared to the mutant, indicating that the (α+β) domain is crucial for the structural rigidity and thermal stability of the intact protein.

3.3. Computational analysis

In order to compare the amino acid sequences of ChiA, ChiB, ChiC and ChiAΔ(α+β), we attempted to align the amino acid sequences of their entire catalytic domains, available from the protein data banks. The alignment obtained by ClustalX was optimized by considering the structural alignment of ChiA and ChiB, as described in the Materials and methods, resulting in a satisfying outcome (Fig. 5). Of particular interest is the region corresponding to the sequence between the seventh and eighth β-strands. This sequence (marked by black letters in Fig. 5) corresponds to the deleted (α+β) domain, which, as it is clearly depicted, is also absent in ChiC. The respective region of ChiB (295–376 aa) is co-aligned with the (α+β) domain of ChiA. The inserted glycine residue, inside the sequence of ChiAΔ(α+β), is marked by the black, small letter "g" in Fig. 5. The gap of the deleted (α+β) domain along the sequence of ChiAΔ(α+β) is aligned with a corresponding gap in the sequence of ChiC.

Molecular modelling, with the use of the "WHATIF" software, revealed that the deletion of the (α+β) domain should have influenced the number of intramolecular side chain interactions, particularly around the region of the catalytic site. It has been calculated that the truncated protein could form 115 fewer potential hydrogen bonds and 20 fewer potential salt bridges, compared to the intact enzyme. These data strongly support our DSC and CD findings, suggesting that ChiAΔ(α+β) must be less rigid and compact than ChiA.

3.4. Enzyme characterization

Enzyme assays were performed by real time measurements of enzymatic degradation of 4MU$(NAG)_2$ and 4MU$(NAG)_3$, as described in the Materials and methods. In spite of their well known disadvantages [48], fluorogenic substrates are indispensable, thanks to their high sensitivity and they were initially used due to the intrinsic difficulties in detecting the enzymatic activity of ChiA-Δ(α+β). After detailed calibration, the concentration of ChiA was determined at 8×10^{-3} μM, whereas the concentration of ChiAΔ(α+β) at 450×10^{-3} μM, in an effort to avoid precipitation of the truncated enzyme. The concentration of both 4MU$(NAG)_2$ and 4MU$(NAG)_3$ was 5 μM in every case. Under these conditions, pH and temperature profiles of both enzymes on 4MU$(NAG)_3$ were obtained. ChiAΔ(α+β) was found to be efficiently active over a much narrower pH range,

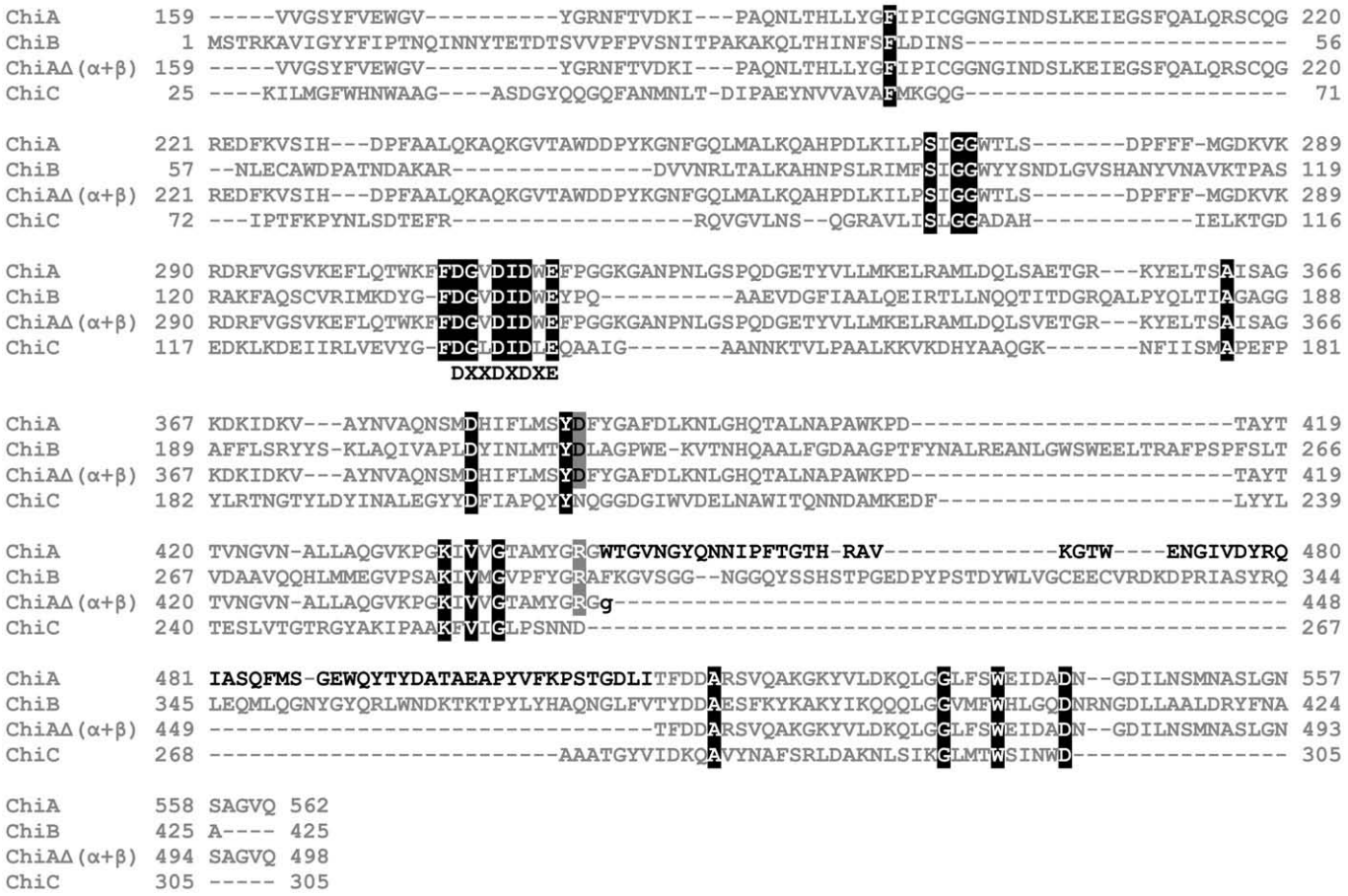

Fig. 5. Amino acid sequence alignment of the catalytic domains of ChiA, ChiB, ChiAΔ(α+β) and ChiC from *S. marcescens*. The overall conserved amino acid residues are boxed in black. The signature of family 18 chitinases is presented by the sequence DXXDXDXE. Asp391, in both ChiA and ChiAΔ(α+β), and co-aligned Asp215 in ChiB are marked by black letters in grey boxes. Arg446, in both ChiA and ChiAΔ(α+β), and co-aligned Arg294 in ChiB are pinpointed by using white letters in grey boxes.

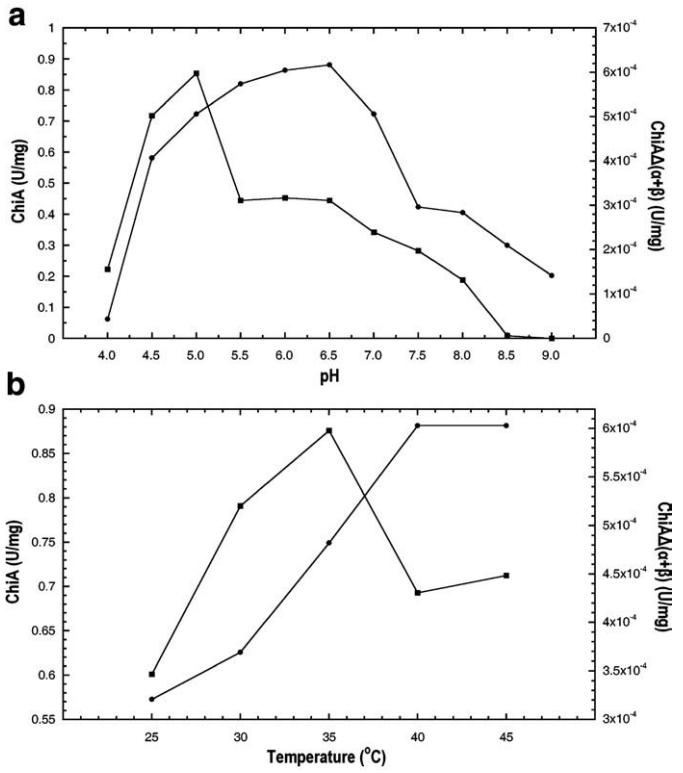

Fig. 6. Enzymatic parameters of ChiA and ChiAΔ(α+β). Dependencies of the enzymatic activity of ChiA (●) and ChiAΔ(α+β) (■) on pH (a) and temperature (b) upon degradation of 4MU$(NAG)_3$. Due to technical limitations, data for temperatures above 45 °C could not be obtained (experimental details in the Materials and methods).

around 5.0, and temperature range, with an optimum of 35 °C, while the native enzyme performs efficiently in a broader pH range (5.5–7.5, with an optimum at 6.5) and a temperature optimum of about 45 °C (Fig. 6a and b). This is in accordance with our DSC and CD results, which indicate predominant alterations of the tertiary structure of ChiAΔ(α+β) at 38 °C (Fig. 2, upper and lower panels). ChiA presented the same pH and temperature profiles upon degradation of both, 4MU$(NAG)_3$ and 4MU$(NAG)_2$.

In contrast, ChiAΔ(α+β) showed no detectable activity towards 4MU$(NAG)_2$ under any combination of pH and temperature conditions. Nonetheless, the truncated protein degraded 4MU$(NAG)_3$, displaying both qualitative and quantitative differences compared to the wild type (Fig. 6a and b). Comparison of the specific activities of ChiA and ChiAΔ(α+β) towards 4MU$(NAG)_3$ clearly revealed a great reduction (about 1.5×10^3 fold) on the catalytic activity of the latter. Moreover, preliminary enzyme kinetics, measuring both catalytic and chitin binding activity, suggest that, although ChiAΔ(α+β) retains a significant potential of chemical affinity towards small chitooligosaccharides, it sustains a great loss in catalytic activity towards these same chitin derivatives.

The enzymatic activity of ChiAΔ(α+β) towards chitin and NAGs of various degrees of polymerization was also investigated. The reactions were carried out as described in the Materials and methods at pH 5.0 and after 48 h the products were analysed by HPLC. While ChiA effectively converts colloidal chitin to $(NAG)_2$ as the primary product and to NAG and $(NAG)_3$ as by-products, ChiAΔ(α+β) poorly digests colloidal chitin to $(NAG)_7$, $(NAG)_6$ and $(NAG)_5$ (Fig. 7). Chitooligosaccharides smaller than $(NAG)_5$ were not detected. Interestingly, when synthetic $(NAG)_7$, $(NAG)_6$, $(NAG)_5$, $(NAG)_4$ and $(NAG)_3$ were used, we could only detect degradation products for $(NAG)_7$ and $(NAG)_6$. $(NAG)_7$ was digested to $(NAG)_6$ and NAG and also to $(NAG)_5$ and $(NAG)_2$, while $(NAG)_6$ was digested to $(NAG)_4$ and $(NAG)_2$. Due to the low specific activity of the truncated enzyme and its instability over long periods of time at its optimum catalytic conditions, quantitative measurements for chitin or chitin oligopolymers degradation are unattainable by the most common methodologies, i.e. TLC analysis [49,50], detection of the reducing saccharides [51] and even via HPLC analysis.

4. Discussion

ChiA from *S. marcescens* is the first bacterial chitinolytic enzyme to be thoroughly studied [13,14]. ChiA is a chitinolytic enzyme of high catalytic activity and specificity and able to degrade insoluble chitin and its soluble derivatives, up to disaccharides, over both wide pH (4.5–8.0) and temperature ranges (25–55 °C). The X-ray structure of ChiA has been determined at high resolution [22–24]; however the function of its individual structural domains, in terms of their contribution to the structural and enzymatic properties of the molecule, remains to be elucidated. According to the crystal structure of ChiA [24], an (α+β) domain is inserted into the main catalytic TIM-barrel domain, between strand B7 and helix A7. This inserted domain, which structurally resembles an almost spherical element, much like a bump, is located directly above the one side of the deep catalytic cleft

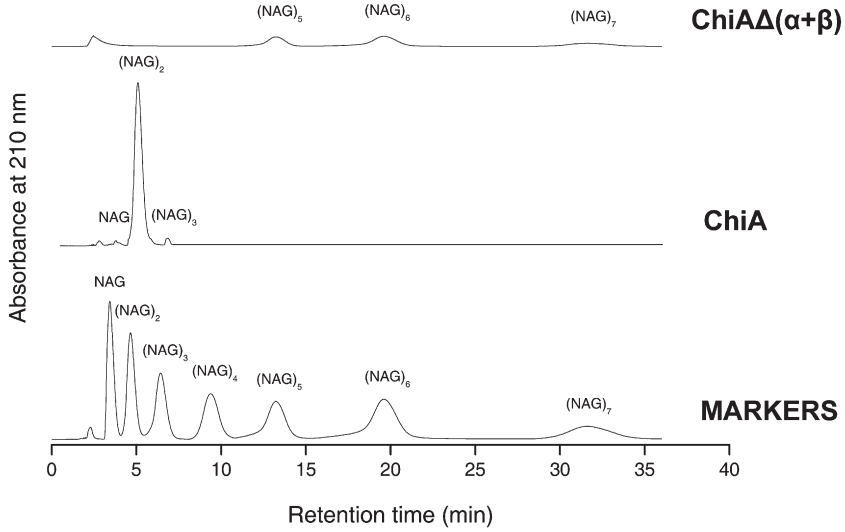

Fig. 7. HPLC analysis of chitin hydrolysis products. ChiA (middle section) and ChiAΔ(α+β) (upper section) were incubated with colloidal chitin, under conditions described in the Materials and methods. The respective hydrolysis products were determined by comparison to standard chitooligosaccharides (lower section).

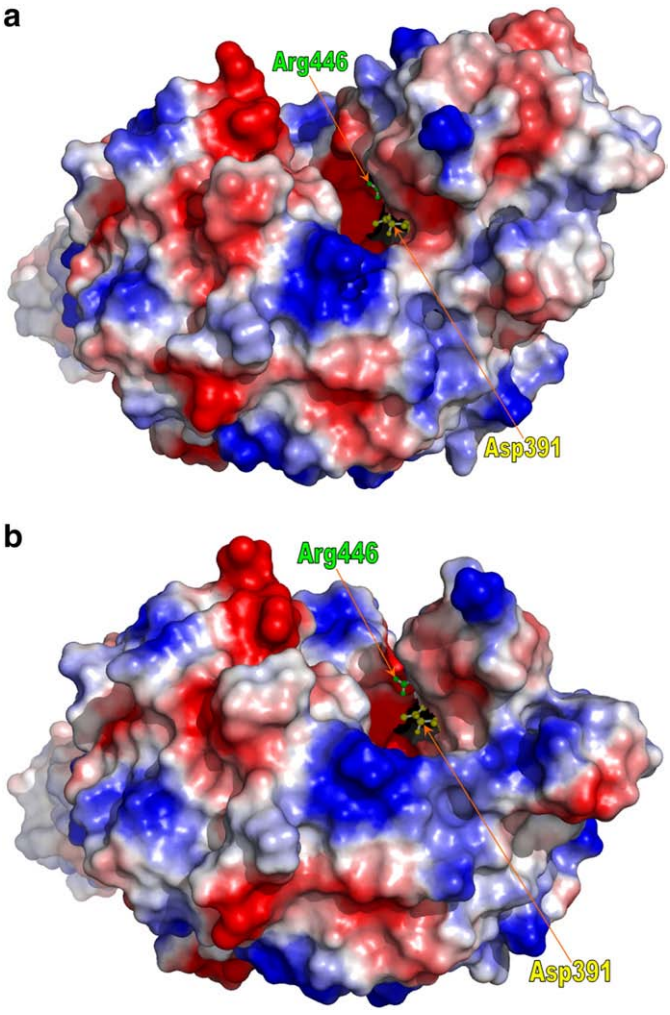

Fig. 8. Space filling models of ChiA and ChiAΔ(α+β). The crystallographic data of ChiA were used in building its model (a) and subsequently the ChiAΔ(α+β) model (b), by homologous modelling, as described in the Materials and methods. Both images illustrate the local electrostatic charges of the two molecules, from those most negative (intense red regions), to those most positive (intense blue regions). Asp391 and Arg446 are partly depicted by yellow and green balls and sticks, respectively.

of the enzyme, contributing to the formation of a tunnel-like active site (Fig. 8a). Structural and enzymatic studies on the mode of action of ChiA and ChiB clearly suggest that the tunnel-like shape of the catalytic cleft facilitates the processive N,N′-di(acetyl)-glycosaminidase (ChiA, ChiB) and the non-processive N,N′,N″-tri(acetyl)-glycosaminidase (ChiB) activity and restrains the non-processive endochitinase activity [4,15,27,29]. In the case of ChiA, the functional contribution of the (α+β)-inserted domain is not clear. Structural elements that are inserted in TIM-barrels have been reported several times, but none has been extensively studied, up to date, possibly due to intrinsic difficulties [11,24,52–54].

In this study we investigated the role of the (α+β) domain on the catalytic activity, specificity and structural stability of ChiA. ChiA is a suitable protein for these studies, since adequate biochemical and structural information is currently available.

By employing genetic engineering technology, we were able to delete the (α+β) domain from the catalytic TIM-barrel domain of ChiA. A targeted insertion of a glycine residue, connecting the two sides of the deletion area, was designed to slightly increase the local structural flexibility of the molecule and prevent possible structural constrains. The recombinant ChiAΔ(α+β) was overproduced in *E. coli* and showed higher solubility when induced at a lower temperature (18 °C). The purified ChiAΔ(α+β) is correctly folded, as indicated when compared to ChiA via CD spectroscopy. However, the thermal stability of the truncated protein was substantially reduced. Microcalorimetric studies of ChiA and ChiAΔ(α+β), in combination with CD spectroscopy, are in agreement and clearly show that the removal of the (α+β) domain from ChiA causes a reduction of the apparent T_m by nearly 20 °C. The fact that the thermal unfolding of both ChiA and ChiAΔ(α+β) is irreversible, does not allow us to precisely calculate the thermodynamic parameters for these molecules. Our current data clearly indicate that the (α+β) domain stabilizes the catalytic TIM-barrel domain of ChiA.

Molecular modelling of ChiAΔ(α+β), based on the crystal structure of ChiA, reveals the structural alterations around the catalytic site, caused by the removal of the (α+β) domain. As demonstrated in Fig. 8a, in ChiA the presence of the (α+β) domain extends the height of the one side of the catalytic groove walls, thus contributing to the formation of a tunnel-shaped catalytic structure. The structure of the active site of ChiA enhances not only the exo-N,N′-di(acetyl)-glycosaminidase activity, but especially promotes the processivity during the degradation of the chitopolymeric chains [29,55–57]. The calculated model of ChiAΔ(α+β) reveals a catalytic domain with a shallow groove, in comparison to the respective groove of ChiA, as illustrated in Fig. 8b, very similar to the suggested structure of ChiC [10,15]. Images of both ChiA and ChiAΔ(α+β) (Fig. 8a and b) show the end of the catalytic cleft, from where the hydrolysis products exit, viewed from exactly the same angle.

ChiC acts almost exclusively as a non-processive endochitinase and its primary structure reveals no additional insertion within its catalytic domain [58]. Sequence alignment data of ChiC imply that due to the absence of an insertion localized near its catalytic site, a similar open and shallow groove is formed [10]. On the other hand, ChiB from *S. marcescens*, previously identified as a processive exochitinase, is characterized by a tunnel-shaped catalytic cleft, very similar to that of ChiA [11,26,28,56,59]. Considering all the observations mentioned above, it can be proposed that the catalytic area of ChiAΔ(α+β) resembles the catalytic domain of ChiC [10,15].

This structural alteration is clearly reflected on the substrate specificity of ChiAΔ(α+β). The chitin degradation pattern deriving from the ChiAΔ(α+β) activity is a mixture of approximately equal amounts of NAGs with respective polymerization sizes 5, 6 and 7, as resolved by our HPLC analysis. Therefore, the truncated enzyme appears to act randomly and non-processively on chitin fibers. These findings are also supported by data obtained by digesting various synthetic NAGs with ChiAΔ(α+β), since the products had various lengths of approximately equal amounts. The degradation of only the longer NAG oligopolymers, $(NAG)_6$ and $(NAG)_7$, also supports the suggestion that ChiAΔ(α+β) is characterized by an endochitinase activity and a preference towards longer chitinous substrates.

Furthermore, our kinetic studies, by use of fluorogenic synthetic substrates, revealed distinct differences in enzyme activity and substrate interactions between the native protein and the truncated one. Upon the deletion of the (α+β) domain, the pH and temperature profiles of ChiA were affected. In addition, the specific activity of ChiAΔ(α+β), compared to that of ChiA, was reduced by nearly 3 orders of magnitude towards $4MU(NAG)_3$ and was totally lost towards $4MU(NAG)_2$.

From the primary structures of ChiA and ChiAΔ(α+β), we were able to calculate, in silico, their theoretical isoelectric points, i.e. 5.73 and 6.36 respectively. These calculations reveal that the (α+β) domain is strongly acidic and therefore reduces the overall theoretical pI of the enzyme by 0.63 pH units. It is profound that the existence of this domain, in proximity to the active site, provides a more acidic microenvironment around E315, which is the proton donor to the saccharide intermediate during the hydrolysis reaction, thereby aiding in maintaining this amino acid residue in its protonated-active state. This is also supported by the pKa predictions, calculated for both proteins by the H+ suite [60]. As a

result, a global change was predicted on the pKa values and the overall charge of the amino acid residues involved in substrate recognition and the composition of the active site (Fig 8a and b). These findings support not only the low specific activity of the truncated enzyme, but also the nature of its enzymatic products.

As reported in previous publications [11,58,61], Arg294 in ChiB is a major determinant for the pH profile of family 18 chitinases. Arg294 is pinpointed as the amino acid mainly responsible for the shifting and subsequent stabilization of the Asp215 pKa value to a more acidic one. Arg294 and Asp215 in ChiB are the counterparts of Arg446 and Asp391 in ChiA, respectively (Fig. 5). Therefore, it can be assumed that Arg446 affects the pKa of Asp391 in ChiA in a similar manner. Arg 446 in ChiA is adjacent to the area from which the $(\alpha+\beta)$ domain is removed (Fig. 8a and b). This structural change could influence the conformation of the side chain of Arg446 and therefore, by affecting Asp391, to change the pH profile of ChiA$\Delta(\alpha+\beta)$ compared to that of ChiA. According to our alignment, ChiC lacks both the respective Asp and Arg residues (Fig. 5) and this fact could explain the similarity of the ChiA$\Delta(\alpha+\beta)$ and ChiC pH profiles [15].

In conclusion, our data strongly support the significant involvement of the $(\alpha+\beta)$ domain in the thermal stability, specificity and enzymatic activity of ChiA. Deletion of this domain renders the resulted enzyme more similar to ChiC, with respect to the optimum pH, the lack of processivity and the catalytic preference towards longer chitopolymers. In order to further investigate the structural and biochemical properties of ChiA$\Delta(\alpha+\beta)$, detailed enzyme kinetics and X-ray structural analysis, in the presence of various chitooligosaccharides, are required.

Acknowledgements

We would like to thank Dr. George Nounesis, Dr. Achileas Tsortos, Dr. Yannis L. Loukas, Dr. Yannis Dotsikas and Dr. Nikolaos C. Papandreou for their scientific support and helpful discussions. A. C. Zees was financially partly supported by the European Scientific Network “Protein design studies of TIM-barrel enzymes: new active sites for chitinase and triosephosphate isomerase” (4th Framework). S. Pyrpassopoulos was financially supported in part by the Graduate Fellowship Program of CSR Demokritos.

References

[1] R.A.A. Muzzarelli, M.G. Peter, Chitin Handbook, European Chitin Society, Grottammare, Italy, 1997.
[2] M.B. Howard, N.A. Ekborg, R.M. Weiner, S.W. Hutcheson, Detection and characterization of chitinases and other chitin-modifying enzymes, J. Ind. Microbiol. Biotechnol. 30 (2003) 627–635.
[3] R.N. Tharanathan, F.S. Kittur, Chitin-the undisputed biomolecule of great potential, Crit. Rev. Food Sci. Nutr. 43 (2003) 61–87.
[4] B. Henrissat, G. Davies, Structural and sequence-based classification of glycoside hydrolases, Curr. Opin. Struct. Biol. 7 (1997) 637–644.
[5] B. Henrissat, G.J. Davies, Glycoside hydrolases and glycosyltransferases. Families, modules, and implications for genomics, Plant Physiol. 124 (2000) 1515–1519.
[6] R. Cohen-Kupiec, I. Chet, The molecular biology of chitin digestion, Curr. Opin. Biotechnol. 9 (1998) 270–277.
[7] T. Ohno, S. Armand, T. Hata, N. Nikaidou, B. Henrissat, M. Mitsutomi, T. Watanabe, A modular family 19 chitinase found in the prokaryotic organism *Streptomyces griseus* HUT 6037, J. Bacteriol. 178 (1996) 5065–5070.
[8] A. Perrakis, K.S. Wilson, I. Chet, A.B. Oppenheim, C.E. Vorgias, Phylogenetic relationships of chitinases, in: R.A.A. Muzzarelli (Ed.), Chitin Enzymology, European Chitin Society, Grottammare, Italy, 1993, pp. 417–422.
[9] M.B. Brurberg, I.F. Nes, V.G. Eijsink, Comparative studies of chitinases A and B from *Serratia marcescens*, Microbiology 142 (Pt 7) (1996) 1581–1589.
[10] K. Suzuki, M. Taiyoji, N. Sugawara, N. Nikaidou, B. Henrissat, T. Watanabe, The third chitinase gene (chiC) of *Serratia marcescens* 2170 and the relationship of its product to other bacterial chitinases, Biochem. J. 343 (Pt 3) (1999) 587–596.
[11] D.M. van Aalten, B. Synstad, M.B. Brurberg, E. Hough, B.W. Riise, V.G. Eijsink, R.K. Wierenga, Structure of a two-domain chitotriosidase from *Serratia marcescens* at 1.9-A resolution, Proc. Natl. Acad. Sci. U. S. A. 97 (2000) 5842–5847.
[12] J. Monreal, E.T. Reese, The chitinase of *Serratia marcescens*, Can. J. Microbiol. 15 (1969) 689–696.
[13] K.J. Downing, G. Leslie, J.A. Thomson, Biocontrol of the sugarcane borer *Eldana saccharina* by expression of the *Bacillus thuringiensis* cry1Ac7 and *Serratia marcescens* chiA genes in sugarcane-associated bacteria, Appl. Environ. Microbiol. 66 (2000) 2804–2810.
[14] K.J. Downing, J.A. Thomson, Introduction of the *Serratia marcescens* chiA gene into an endophytic *Pseudomonas fluorescens* for the biocontrol of phytopathogenic fungi, Can. J. Microbiol. 46 (2000) 363–369.
[15] K. Suzuki, N. Sugawara, M. Suzuki, T. Uchiyama, F. Katouno, N. Nikaidou, T. Watanabe, Chitinases A, B, and C1 of *Serratia marcescens* 2170 produced by recombinant *Escherichia coli*: enzymatic properties and synergism on chitin degradation, Biosci., Biotechnol., Biochem. 66 (2002) 1075–1083.
[16] I. Tews, R. Vincentelli, C.E. Vorgias, N-acetylglucosaminidase (chitobiase) from *Serratia marcescens*: gene sequence, and protein production and purification in *Escherichia coli*, Gene 170 (1996) 63–67.
[17] G. Vaaje-Kolstad, S.J. Horn, D.M. van Aalten, B. Synstad, V.G. Eijsink, The non-catalytic chitin-binding protein CBP21 from *Serratia marcescens* is essential for chitin degradation, J. Biol. Chem. 280 (2005) 28492–28497.
[18] T. Watanabe, K. Kimura, T. Sumiya, N. Nikaidou, K. Suzuki, M. Suzuki, M. Taiyoji, S. Ferrer, M. Regue, Genetic analysis of the chitinase system of *Serratia marcescens* 2170, J. Bacteriol. 179 (1997) 7111–7117.
[19] N. Nagano, C.A. Orengo, J.M. Thornton, One fold with many functions: the evolutionary relationships between TIM barrel families based on their sequences, structures and functions, J. Mol. Biol. 321 (2002) 741–765.
[20] R.K. Wierenga, The TIM-barrel fold: a versatile framework for efficient enzymes, FEBS Lett. 492 (2001) 193–198.
[21] T. Watanabe, K. Kobori, K. Miyashita, T. Fujii, H. Sakai, M. Uchida, H. Tanaka, Identification of glutamic acid 204 and aspartic acid 200 in chitinase A1 of *Bacillus circulans* WL-12 as essential residues for chitinase activity, J. Biol. Chem. 268 (1993) 18567–18572.
[22] Y. Papanikolau, G. Prag, G. Tavlas, C.E. Vorgias, A.B. Oppenheim, K. Petratos, High resolution structural analyses of mutant chitinase A complexes with substrates provide new insight into the mechanism of catalysis, Biochemistry 40 (2001) 11338–11343.
[23] Y. Papanikolau, G. Tavlas, C.E. Vorgias, K. Petratos, De novo purification scheme and crystallization conditions yield high-resolution structures of chitinase A and its complex with the inhibitor allosamidin, Acta Crystallogr., D: Biol. Crystallogr. 59 (2003) 400–403.
[24] A. Perrakis, I. Tews, Z. Dauter, A.B. Oppenheim, I. Chet, K.S. Wilson, C.E. Vorgias, Crystal structure of a bacterial chitinase at 2.3 A resolution, Structure 2 (1994) 1169–1180.
[25] N.N. Aronson Jr., B.A. Halloran, M.F. Alexyev, L. Amable, J.D. Madura, L. Pasupulati, C. Worth, P. Van Roey, Family 18 chitinase-oligosaccharide substrate interaction: subsite preference and anomer selectivity of *Serratia marcescens* chitinase A, Biochem. J. 376 (2003) 87–95.
[26] Y. Honda, M. Kitaoka, K. Tokuyasu, C. Sasaki, T. Fukamizo, K. Hayashi, Kinetic studies on the hydrolysis of N-acetylated and N-deacetylated derivatives of 4-methylumbelliferyl chitobioside by the family 18 chitinases ChiA and ChiB from *Serratia marcescens*, J. Biochem. (Tokyo) 133 (2003) 253–258.
[27] S.J. Horn, A. Sorbotten, B. Synstad, P. Sikorski, M. Sorlie, K.M. Varum, V.G. Eijsink, Endo/exo mechanism and processivity of family 18 chitinases produced by *Serratia marcescens*, FEBS J. 273 (2006) 491–503.
[28] E.L. Hult, F. Katouno, T. Uchiyama, T. Watanabe, J. Sugiyama, Molecular directionality in crystalline beta-chitin: hydrolysis by chitinases A and B from *Serratia marcescens* 2170, Biochem. J. 388 (2005) 851–856.
[29] P. Sikorski, A. Sorbotten, S.J. Horn, V.G. Eijsink, K.M. Varum, *Serratia marcescens* chitinases with tunnel-shaped substrate-binding grooves show endo activity and different degrees of processivity during enzymatic hydrolysis of chitosan, Biochemistry 45 (2006) 9566–9574.
[30] J.D. Jones, K.L. Grady, T.V. Suslow, J.R. Bedbrook, Isolation and characterization of genes encoding two chitinase enzymes from *Serratia marcescens*, EMBO J. 5 (1986) 467–473.
[31] J. Sambrook, E.F. Fritsch, T. Maniatis, Molecular cloning, A Laboratory Manual (2nd Edition). 2nd ed., Cold Spring Harbor Laboratory Press, Cold Spring Harbor, USA, 1989.
[32] F. Sanger, S. Nicklen, A.R. Coulson, DNA sequencing with chain-terminating inhibitors, Proc. Natl. Acad. Sci. U. S. A. 74 (1977) 5463–5467.
[33] F.W. Studier, A.H. Rosenberg, J.J. Dunn, J.W. Dubendorff, Use of T7 RNA polymerase to direct expression of cloned genes, Methods Enzymol. 185 (1990) 60–89.
[34] U.K. Laemmli, Cleavage of structural proteins during the assembly of the head of bacteriophage T4, Nature 227 (1970) 680–685.
[35] M.M. Bradford, A rapid and sensitive method for the quantitation of microgram quantities of protein utilizing the principle of protein-dye binding, Anal. Biochem. 72 (1976) 248–254.
[36] S.C. Gill, P.H. von Hippel, Calculation of protein extinction coefficients from amino acid sequence data, Anal. Biochem. 182 (1989) 319–326.
[37] C.N. Pace, F. Vajdos, L. Fee, G. Grimsley, T. Gray, How to measure and predict the molar absorption coefficient of a protein, Protein Sci. 4 (1995) 2411–2423.
[38] H. Towbin, T. Staehelin, J. Gordon, Electrophoretic transfer of proteins from polyacrylamide gels to nitrocellulose sheets: procedure and some applications, Proc. Natl. Acad. Sci. U. S. A. 76 (1979) 4350–4354.
[39] M. O'Brien, R.R. Colwell, A rapid test for chitinase activity that uses 4-methylumbelliferyl-N-acetyl-beta-D-glucosaminide, Appl. Environ. Microbiol. 53 (1987) 1718–1720.
[40] Y. Yang, K. Hamaguchi, Hydrolysis of 4-methylumbelliferyl N-acetyl-chitotrioside catalyzed by hen and turkey lysozymes. pH dependence of the kinetics constants, J. Biochem. (Tokyo) 87 (1980) 1003–1014.
[41] J.D. Thompson, T.J. Gibson, F. Plewniak, F. Jeanmougin, D.G. Higgins, The CLUSTAL_X windows interface: flexible strategies for multiple sequence alignment aided by quality analysis tools, Nucleic Acids Res. 25 (1997) 4876–4882.

[42] M.A. Marti-Renom, A.C. Stuart, A. Fiser, R. Sanchez, F. Melo, A. Sali, Comparative protein structure modeling of genes and genomes, Annu. Rev. Biophys. Biomol. Struct. 29 (2000) 291–325.
[43] L. Holm, C. Sander, Protein structure comparison by alignment of distance matrices, J. Mol. Biol. 233 (1993) 123–138.
[44] G. Vriend, WHAT IF: a molecular modeling and drug design program, J. Mol. Graphics 8 (1990) 52–56 29.
[45] D. Petrey, B. Honig, GRASP2: visualization, surface properties, and electrostatics of macromolecular structures and sequences, Methods Enzymol. 374 (2003) 492–509.
[46] K.P. Murphy, E. Freire, Thermodynamics of structural stability and cooperative folding behavior in proteins, Adv. Protein Chem. 43 (1992) 313–361.
[47] J.M. Sanchez-Ruiz, Theoretical analysis of Lumry–Eyring models in differential scanning calorimetry, Biophys. J. 61 (1992) 921–935.
[48] I.M. Krokeide, B. Synstad, S. Gaseidnes, S.J. Horn, V.G. Eijsink, M. Sorlie, Natural substrate assay for chitinases using high-performance liquid chromatography: a comparison with existing assays, Anal. Biochem. 363 (2007) 128–134.
[49] E. Kamst, K.M. van der Drift, J.E. Thomas-Oates, B.J. Lugtenberg, H.P. Spaink, Mass spectrometric analysis of chitin oligosaccharides produced by Rhizobium NodC protein in *Escherichia coli*, J. Bacteriol. 177 (1995) 6282–6285.
[50] R.F. Powning, H. Irzykiewicz, Separation of chitin oligosaccharides by thin-layer chromatography, J. Chromatogr. 29 (1967) 115–119.
[51] T. Imoto, K. Yagishita, A simple activity measurement of lysozyme, Agric. Biol. Chem. 35 (1971) 1154–1156.
[52] D.B. Srivastava, A.S. Ethayathulla, J. Kumar, N. Singh, S. Sharma, U. Das, A. Srinivasan, T.P. Singh, Crystal structure of a secretory signalling glycoprotein from sheep at 2.0A resolution, J. Struct. Biol. 156 (2006) 505–516.
[53] J. Kumar, A.S. Ethayathulla, D.B. Srivastava, S. Sharma, S.B. Singh, A. Srinivasan, M.P. Yadav, T.P. Singh, Structure of a bovine secretory signalling glycoprotein (SPC-40) at 2.1 Angstrom resolution, Acta Crystallogr., D: Biol. Crystallogr. 62 (2006) 953–963.
[54] H.J. Flint, T.R. Whitehead, J.C. Martin, A. Gasparic, Interrupted catalytic domain structures in xylanases from two distantly related strains of *Prevotella ruminicola*, Biochim. Biophys. Acta 1337 (1997) 161–165.
[55] S. Cottaz, B. Brasme, H. Driguez, A fluorescence-quenched chitopentaose for the study of endo-chitinases and chitobiosidases, Eur. J. Biochem. 267 (2000) 5593–5600.
[56] G. Davies, B. Henrissat, Structures and mechanisms of glycosyl hydrolases, Structure 3 (1995) 853–859.
[57] T. Uchiyama, F. Katouno, N. Nikaidou, T. Nonaka, J. Sugiyama, T. Watanabe, Roles of the exposed aromatic residues in crystalline chitin hydrolysis by chitinase A from *Serratia marcescens* 2170, J. Biol. Chem. 276 (2001) 41343–41349.
[58] B. Synstad, G. Vaaje-Kolstad, F.H. Cederkvist, S.F. Saua, S.J. Horn, V.G. Eijsink, M. Sorlie, Expression and characterization of endochitinase C from *Serratia marcescens* BJL200 and its purification by a one-step general chitinase purification method, Biosci. Biotechnol. Biochem. 72 (2008) 715–723.
[59] D.M. van Aalten, D. Komander, B. Synstad, S. Gaseidnes, M.G. Peter, V.G. Eijsink, Structural insights into the catalytic mechanism of a family 18 exo-chitinase, Proc. Natl. Acad. Sci. U. S. A. 98 (2001) 8979–8984.
[60] J.C. Gordon, J.B. Myers, T. Folta, V. Shoja, L.S. Heath, A. Onufriev, H+: a server for estimating pKas and adding missing hydrogens to macromolecules, Nucleic Acids Res. 33 (2005) W368–W371.
[61] B. Synstad, S. Gaseidnes, D.M. Van Aalten, G. Vriend, J.E. Nielsen, V.G. Eijsink, Mutational and computational analysis of the role of conserved residues in the active site of a family 18 chitinase, Eur. J. Biochem. 271 (2004) 253–262.